Asian Journal of Chemistry; Vol. 24, No. 11 (2012), 5264-5268

ASIAN JOURNAL OF CHEMISTRY

www.asianjournalofchemistry.co.in

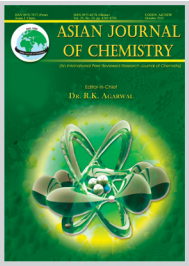

Synthesis, Characterization, Antimicrobial and Antiinflammatory Effect of Chitosan/Hydroxyapatite Nanocomposite

C.P. DHANALAKSHMI[1], L. VIJAYALAKSHMI[2] and V. NARAYANAN[1,*]

[1]Department of Inorganic Chemistry, University of Madras, Guindy Maraimalai Campus, Chennai-600 025, India
[2]Department of Chemistry, S.D.N.B. Vaishnav College for Women, Chrompet, Chennai-600 044, India

*Corresponding author: E-mail: vnnara@yahoo.co.in

(*Received*: 15 October 2011; *Accepted*: 15 June 2012) AJC-11611

Chitosan/hydroxyapatite nanocomposites of varying composition for biomaterial applications have been synthesized by wet chemical method. The Chitosan/hydroxyapatite nanocomposite materials were characterized by XRD, FTIR, ^{31}P NMR and FESEM. Hydroxyapatite (HAp) nanorod embedded composite was prepared using chitosan as a matrix with different weight percentages (wt %). The results indicated that the size and crystallinity of hydroxyapatite nano particles decreases with increase in chitosan concentration in the composite. SEM confirms the presence of hydroxyapatite nanorod crystals in chitosan (CHS) matrix, chitosan/hydroxyapatite. The nano composites were screened for antimicrobial activity and also for antiinflammatory activity.

Key Words: Hydroxyapatite, Nanocomposite, Chitosan, Antimicrobial activity, Antiinflammatory activity.

INTRODUCTION

Synthetic hydroxyapatite has been used extensively for biomedical implant applications and bone regeneration due to its bioactive and osteoconductive properties[1]. In addition, hydroxyapatite can accelerate the formation of bonelike apatite on the surface of the implant[2]. Owing to its brittleness, the instability of the hydroxyapatite particulate is often encountered when the particles are mixed with saline or patient's blood, making it unable to be used as bone regenerating template. To solve the problem, incorporation of hydroxyapatite into polymer matrix has been carried out to increase osteoconductivity and biodegradabilty with significant enhancement of mechanical strength. Chitosan (CHS) can be utilized in combination with hydroxyapatite to meet these requirements. Chitosan is one of the most widely-used natural polymers in tissue engineering research that can be obtained by partial deacetylation of chitin which can be extracted from shells of crustacean (prawns, crab, squids, *etc.*). Many forms of chitosan/hydroxyapatite nano composites have been synthesized such as powder form, membrane, pastes, cements, microsphere and scaffolds. The chitosan/hydroxyapatite nano composite was prepared by mechanical mixing[3] or *in situ* precipication[4]. Nano size hydroxyapatite was found to enhance the growth of apatite on the composite scaffolds. In this study the nano hydroxyapatite was synthesized and mixed with chitosan (CHS) in different percentage to form chitosan/hydroxyapatite nano composites. This polymer attracts a particular attention in the development of biomaterial composites because this natural polysaccharide derived from chitin after N-deacetylation is biodegradable and biocompatible. This polymer has been largely used in biomedical applications especially as scaffolds. Ideally, the scaffolds should have a high porosity, a large specific area, a suitable pore size and a highly interconnected pore structure to provide enough space for the tissue development and to promote neovascularization[5]. This porosity can also control inorganic crystal nucleation, growth, microstructure and more generally the properties of such mineral-based materials. Therefore, several preparation methods have been reported for porous scaffolds, including porogen leaching[6], saturation and release of CO_2[7] and traditional phase separation technique[8]. A widely used method is freeze-drying (freezing at -80 ºC), which is a thermally induced phase separation (TIPS)[9].

The addition of nano sized particles is desirable to develop the composite with a good mechanical strength since the natural bone contains mineral crystals which are at the nanometer scale and embedded in the collagen matrix[10]. The polymer composites are designed to meet the specific requirement of biomedical applications like tissue engineering and drug delivery system. The right choice of the composition of both filler and polymer matrix are essential in addition to the process method to obtain suitable biopolymer composites. Recently, attempts have been made to develop nano composites,

wherein nano hydroxyapatite particles are embedded in chitosan polymeric matrices[10-12].

An extensive study have been made on both natural (chitosan, collagen, gelatin, silk fibroin) and synthetic (polyethylene, polyamide, polystyrene, poly(vinyl alcohol), poly(ethylene glycol) and poly(etheretherketone)) polymers to overcome the mechanical problems associated with bio ceramics in bone tissue engineering applications[13-16]. Among the above polymers, chitosan remains one of the widely used polymer group of biomaterials applied for medical implants. This wide range of versatility is utilized in terms of tailoring their applications such as tissue scaffolding[17], artificial cartilage[18] and biodegradable scaffolds[19-21]. With the superior combination of the synergic effect and biocompatible hydroxyapatite and the adjustable biodegradability of polymer matrix, hydroxyapatite nano rod embedded chitosan composites were prepared under controlled environment. The present work carried out elaborates on synthesis of nano structured hydroxyapatite by wet chemical method using calcium hydroxide and ammonium dihydrogen phosphate as starting materials and synthesis of nano structured chitosan/hydroxyapatite composite by freeze drying method using synthetic nano hydroxyapatite as starting materials with the aid of chitosan. In this paper chitosan/hydroxyapatite nano composites of varying compositions were prepared. This biomaterial will be easy to adhere to tissue and fix in site for a long-term. This composite is a very promising material for use in artificial articular cartilage. In the present work we tried to synthesize, characterize and evaluate the *in vitro* study of antimicrobial and antiinflammatory effect of the chitosan/hydroxyapatite nano composite materials.

EXPERIMENTAL

Analytical grade calcium hydroxide and ammonium dihydrogen phosphate were obtained from Merck. Chitosan was purchased from Loba and used. Doubly distilled water was used as the solvent.

Synthesis of nano hydroxyapatite: The nano hydroxyapatite was synthesized by following a modified wet chemical method. At 25 ºC, 7.48 g of $Ca(OH)_2$ was first dissolved in a 100 mL volume of an ethanol-water mixture (50:50 %, v/v) and stirred for 3 h. A solution of 6.7 g $(NH_4)H_2PO_4$ was dissolved in 100 mL volume of water and then added to the $Ca(OH)_2$ solution over a period of 24 h. The amount of reagents in the solution was calculated to obtain a Ca/P molar ratio equals to a 1.67 value, corresponding to a stoichiometric hydroxyapatite. The pH of the slurry was measured during the precipitation reaction, reaching a final value of pH 11.

Synthesis of chitosan/hydroxyapatite nano composites: The chitosan/ hydroxyapatite nano composites were coded as chitosan 10/hydroxyapatite to chitosan 80/hydroxyapatite where number denotes the wt % of chitosan. Water was used as the solvent to prepare polymer solution. Chitosan was dissolved by using magnetic stirrer for 3 h and the polymer solution was left overnight in room temperature to remove the air bubbles trapped in the viscous solution. Then suitable amount of hydroxyapatite was dispersed in deionized water by 30 min ultrasonication. Ultrasonication was necessary to avoid agglomeration of ceramic powder and to achieve proper dispersion. Hydroxyapatite in water was mixed with polymer solution under agitation. The homogeneously mixed solution is immediately taken to deep freeze at -18 ºC. After 48 h freezing the samples were freeze dried.

Characterization: The prepared samples were studied by FTIR spectroscopy using a Shimadzu FT-IR 300 series instrument. The FTIR spectra were obtained over the region 450-4000 cm^{-1} in pellet form for 1 mg powder samples mixed with 200 mg spectroscopic grade KBr. Spectra were recorded at 4 cm^{-1} resolution averaging 80 scans. The structure of the samples were analyzed by a Rich Siefert 3000 diffractometer with $CuK_{\alpha 1}$ radiation (λ = 1.5418 Å). The diffraction peak at 25.9º was chosen for calculation of the crystallite size by Scherrer's formula since it is sharper and isolated from others. This peak assigns to (002) Miller's plane family and shows the crystal growth along the axis of hydroxyapatite crystalline structure. The morphology of the materials was analyzed by FESEM using a HITACHI S600N scanning electron microscopy. For the elemental analysis the electron microscope was equipped with an energy dispersive X-ray attachment. ^{31}P-MAS-NMR spectra were recorded on a Bruker MSL 300 spectrometer equipped with an Andrew type rotor rotating at a frequency of 10 KHz.

RESULTS AND DISCUSSION

XRD analysis: The XRD patterns of the chitosan and chitosan/hydroxyapatite nano composites are shown in Fig. 1. The peak appeared approximately at 21º was assigned to chitosan. The sharp diffraction characteristic peaks appeared at around 32º is for the chitosan/hydroxyapatite nano composites correspond to the peaks of hydroxyapatite powder. This results confirm the existence of hydroxyapatite compound in the chitosan matrix. XRD patterns suggest the presence of nanocrystalline apatite, its crystallinity decreasing with increasing chitosan content (Fig. 1). Diffraction peak broadening is inversely proportional to crystallite size, hence the greater the proportion of chitosan in the composite the smaller the average size of the apatite crystals. Slightly increased intensity of the (002) and (004) peaks compared with the reference data suggests that the apatite crystallites are elongated along the crystallographic axis A (which is characteristic of bone tissue bioapatite).

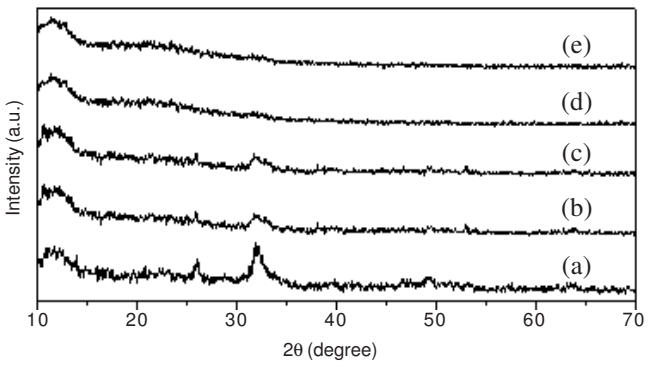

Fig. 1. XRD Pattern of (a) nano hydroxyapatite, (b) nano chitosan 20/ hydroxyapatite, (c) nano chitosan 40/hydroxyapatite, (d) nano chitosan 60/hydroxyapatite and (e) nano chitosan 80/hydroxyapatite

FTIR analysis: From the IR spectroscopy of the different chitosan/hydroxyapatite composites it is inferred that all the major absorbance bands of the spectra correspond to hydroxyapatite; their width increases significantly with increasing chitosan content (Fig. 2). The bands at 1100-1000 cm^{-1} and 600-500 cm^{-1} correspond to different modes of the PO_4^{3-} group in hydroxyapatite. Broadening of the band at 1050 cm^{-1} shows the presence of polymer and its interaction with the phosphate groups[22]. The bands at 1485-1420 cm^{-1} and at about 875 cm^{-1} are due to the carbonate ions in apatite. The bands at 1700-1550 cm^{-1} are attributable to mode super position of the hydroxyapatite OH group and the chitosan amide I and amide II groups. The bands at 3700-3600 cm^{-1} and 2950-2800 cm^{-1} are assigned to the hydroxyl groups present in chitosan[23]. The hydroxyapatite phosphate stretching (vibration) bands are at 1100-1000 cm^{-1} and the phosphate bending bands are at 600-500 cm^{-1}. The strongest characteristic CO_3^{2-} bands are also visible, at 1485-1420 cm^{-1}

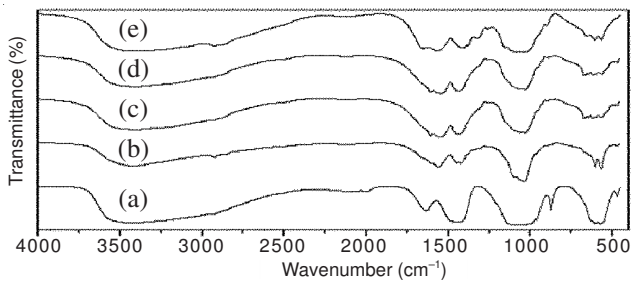

Fig. 2. FTIR Spectrum of (a) nano hydroxyapatite, (b) nano chitosan 20/ hydroxyapatite, (c) nano chitosan 40/hydroxyapatite, d) nano chitosan 60/hydroxyapatite and (e) nano chitosan 80/hydroxyapatite

FE-SEM analysis: SEM images of pure nano hydroxyapatite and different weight percentages of chitosan compositions are illustrated in Fig. 3. The SEM picture shows that particles exhibit nano rod morphology. When all the SEM images of composites are considered highly porous structure was common in all these materials. The smoothest surface at pure chitosan began to be disturbed with incorporation of hydroxyapatite gradually resulting in a rough surface which was not smooth anymore. The hydroxyapatite particles were embedded well in the chitosan matrix. The uniformly distributed hydroxyapatite particles could be seen through the chitosan matrix which have interconnected cells. The pore shape seemed to change with hydroxyapatite, in pure chitosan sample pores were more flat but when hydroxyapatite wt % was only 20, pores became more rounded rather than flat.

^{31}P MAS-NMR analysis: The ^{31}P MAS-NMR spectra for the chitosan/hydroxyapatite nano composite and nano hydroxyapatite powders are shown in Fig. 4. A distinctive resonance peak appears at 2.568 ppm in Fig. 4a for the nano hydroxyapatite. After the development of chitosan/hydroxyapatite nano composites, the ^{31}P characteristic peak moves to 3.142 ppm as shown in Fig. 4b, indicating that after the formation of nano composites, the chemical environment of the phosphorus atom in nano hydroxyapatite crystal has been changed. This shift is due to the interaction of hydroxyapatite with chitosan in chitosan/hydroxyapatite nano composite. The chemical interaction may be due the hydrogen bonding interaction between

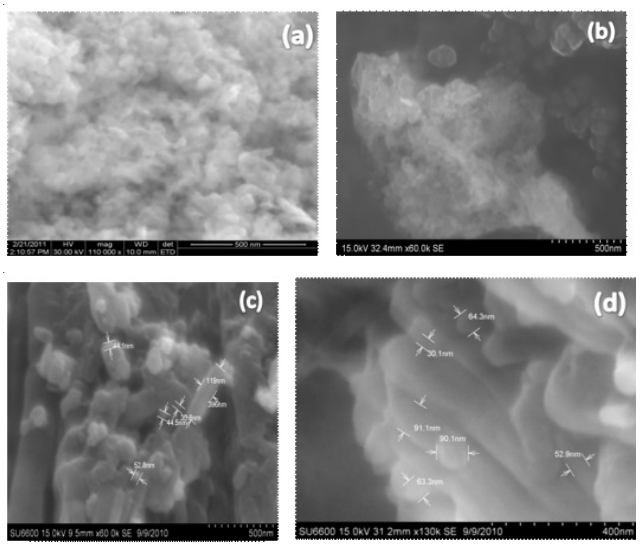

Fig. 3. FE-SEM images of (a) nano hydroxyapatite, (b) nano chitosan 20/ hydroxyapatite, (c) nano chitosan 40/hydroxyapatite and (d) nano chitosan 60/hydroxyapatite

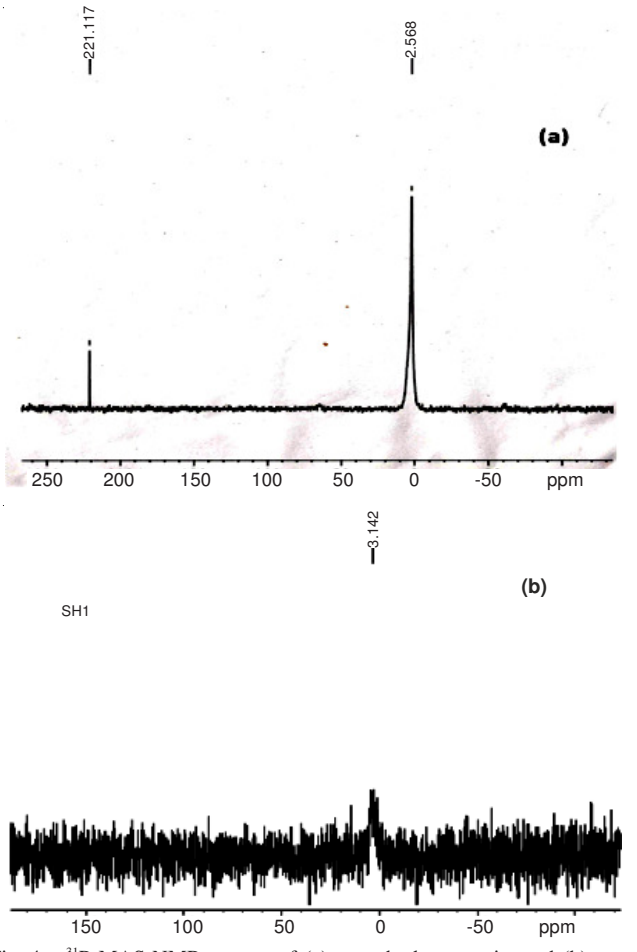

Fig. 4. ^{31}P MAS-NMR spectra of (a) nano hydroxyapatite and (b) nano chitosan 40/hydroxyapatite composite

the PO_4^{3-} ions of hydroxyapatite and the -OH functional groups of chitosan[24].

Antimicrobial activities: Antifungal and antibacterial activities of the chitosan/hydroxyapatite nano composites were tested by the well diffusion method using Sabouraud dextrose agar and Muller Hinton agar[25]. The radial growth of the colony

TABLE-1
ANTIBACTERIAL AND ANTIFUNGAL ACTIVITY OF CHITOSAN/HYDROXYAPATITE NANOCOMPOSITES

Organisms	Sample name Representation of zone of inhibition (diameter in mm)											
	Chitosan 20/hydroxyapatite concentration (µg)			Chitosan 40/hydroxyapatite concentration (µg)			Chitosan 60/hydroxyapatite concentration (µg)			Chitosan 80/hydroxyapatite concentration (µg)		
	500	750	1000	500	750	1000	500	750	1000	500	750	1000
S. aureus	11	12	13	11	11	11	11	11	11	-	-	-
S. typi	-	11	12	13	14	15	12	13	13	13	14	14
E. coli	-	11	12	13	13	14	11	13	14	11	12	13
V. cholerae	11	12	11	11	12	14	-	-	11	11	12	-
K. pneumoniae	-	12	12	11	15	17	12	11	11	-	12	15
C. albicans	11	12	13	-	11	12	-	11	12	11	11	12
C. paratrophicalis	11	12	12	-	11	12	-	11	11	-	11	11

S. aureus = *Staphylococcus aureus* (ATCC 12600); *S. typi* = *Salmonella typi* (ATCC 700931); *E. coli* = *Escherichia coli* (ATCC 11775); *V. cholerae* = *Vibrio cholera* (ATCC 39315); *K. pneumoniae* = *Klebsiella pneumonia* (ATCC 13883); *C. albicans* = *Candida albicans* (ATCC 90028); *C. paratrophicalis* = *Candida paratrophicalis* (ATCC 42618)

was recorded on completion of the incubation and the mean diameter for each composite at a concentration of 250 µg/mL, 500 µg/mL, 750 µg/mL, 1000 µg/mL were recorded. The average percentage inhibition of the bacterial growth medium was compared using the Vincent equation I = 100/(C-T)/C, where I = percentage inhibition, T = average diameter of the bacterial growth on the tested plates and C-average diameter of the growth on the control plates. Stock solutions of tested compounds were prepared in dimethyl sulfoxide.

Inoculum preparation: Fresh bacterial cultures were used for the antibacterial susceptibility test. Five ATCC colonies of the strains were inoculated to Tryptic soy or Brain Heart Infusion broth and incubated at 37 ºC for 22-24 h time period. Turbidity was adjusted with sterile broth so as to correspond to the 0.5 McFarland standard, a standard inoculum of the microorganism 1.5×10^6 colony forming units CFU/mL, a 1:100 dilution of a suspension of turbidity equal to a McFarland 0.5. The turbidity was adjusted to match a McFarland 0.5 barium sulfate method. This is prepared by adding 0.5 mL of of 1.175 % w/v (0.048 m) hydrate ($BaCl_2.2H_2O$) to 99.5 mL of 1 % w/v (0.36) sulfuric acid.

Antifungal activity: We have evaluated the antifungal activity of the chitosan/hydroxyapatite nano composites against the human pathogenic fungus *Candida albicans* and *Candida paratrophicalis*. The screening data for the composites are given in Table-1. It is observed from the results that chitosan/hydroxyapatite nano composite shows some antifungal activity. However the chitosan 20/hydroxyapatite nano composite showed higher activity against the tested fungus at concentration of 1000 µg/mL when compared with the other chitosan/hydroxyapatite nano composite. It is also observed from the study that the chitosan/hydroxyapatite nano composite containing chitosan 20/hydroxyapatite composition shows higher activity than the other chitosan/hydroxyapatite compositions.

Antibacterial activity: All the prepared chitosan/hydroxyapatite nano composites have been screened for their *in vitro* antibacterial activity against selected five pathogenic bacteria such as *Staphylococcus aureus, Escherichia coli, Salmonella. typi, Vibrio cholerae* and *Klebsiella pneumonia* respectively. The screening results of the composites are shown in the Table-1. All the chitosan/hydroxyapatite composition of nano composite shows comparable activity against all the selected bacteria. From the data it is observed that at concentration of 1000 µg/mL, the composite of chitosan 40/hydroxyapatite showed higher antibacterial activity against *Salmonella typi* and *Klebsiella pneumoniae*. Chitosan 60 /hydroxyapatite is also showed higher antibacterial activity against *E. coli*. Chitosan 20/hydroxyapatite is also showed higher antifungal activity against *Candida albicans*. The antibacterial activity is dependent on the molecular structure of the compound, the solvent used and the bacterial strain under consideration.

Antiinflammatory activity by HRBC membrane stabilization method: The HRBC membrane stabilization has been used as a method to study the antiinflammatory activity[26]. Blood was collected from healthy volunteer. The collected blood was mixed with equal volume of sterilized Alsever solution (2 % dextrose, 0.8 % sodium citrate, 0.05 % citric acid and 0.42 % sodium chloride in water). The blood was centrifuged at3000 rpm and packed cell were washed with isosaline (0.85 %, pH 7.2) and a 10 % (v/v) suspension was made with isosaline. The assay mixture contained the drug (various concentrations g/mL), 1 mL of phosphate buffer (0.15 M, pH 7.4), 2 mL of hyposaline (0.36 %) and 0.5 mL of HRBC suspension. Diclofenac was used as reference drug. Instead of hyposaline 2 mL of distilled water was used in the control. All the assay mixture were incubated at 37 ºC for 0.5 h and centrifuged. The hemoglobin content in the supernatant solution was estimated using spectrophotometer at 560 nm. The percentage protection was calculated by assuming the haemolysis produced in presence of distilled water of as 100 %. The percentage of haemolysis was calculated using the formula:

$$\text{Protection}(\%) = \frac{100 - \text{Optical density of drug treated sample}}{\text{Optical density of control}} \times 100$$

The compound chitosan20/hydroxyapatite and chitosan 60/hydroxyapatite showed significant protection towards HRBC membrane rupture which is induced by hypotonic saline. The effect may be due to the resistance caused by polymers in the destruction of erythrocyte membrane. From the results it was proved that chitosan20/hydroxyapatite composition (Table-2) was more effective than chitosan60/hydroxyapatite composition (Table-2) and also chitosan/hydroxyapatite nano composites were more effective than nano hydroxyapatite (Table-2). Further work is in progress to identify the exact mechanism involved in antiinflammatory activity[27].

TABLE-2
ANTIINFLAMMATORY ACTIVITY BY HRBC MEMBRANE STABILIZATION METHOD

Concentration (µg/mL)	Inhibition of HAp (%)	Inhibition of CHS 20/HAp nanocomposite (%)	Inhibition of CHS 60/HAp nanocomposite (%)
1000	93.00	99.12	97.14
800	93.03	99.12	99.21
400	98.67	99.85	98.45
200	98.57	99.90	99.23
100	98.43	99.14	99.44
50	98.72	98.16	98.72
10	99.25	99.52	94.94

CHS = Chitosan; Hap = Hydroxyapatite.

Conclusion

The investigated chitosan/hydroxyapatite nano composite materials have proved to be promising for the treatment of bone defects. In the present work, a novel chitosan/hydroxyapatite nanocomposite is prepared by simple chemical route. The reduction in particle size with increase in concentration of chitosan is due to the size control effect of chitosan molecular structure. The smoothest surface at pure chitosan began to be disturbed with incorporation of hydroxyapatite gradually resulting in a rough surface which was not smooth anymore. It inferred that the composition of chitosan shows significant influence on particle size, antimicrobial and antiinflammatory activities, which facilitate to optimize the composition of composite for particular applications. Nano materials are greatly promising in the development of more valuable orthopedic and dental implants. However, the mechanism of chitosan/nano hydroxyapatite interaction is expected to investigate thoroughly, which will promote the research of bio materials with better biological performance.

ACKNOWLEDGEMENTS

The authors are grateful for the financial supports from the University Grants Commission and Council of Scientific and Industrial Research, New Delhi, India.

REFERENCES

1. J.M. Gomez-Vega, *Biomaterials*, **211**, 285 (2000).
2. A. Sabokbar, R. Pandey, J. Diaz, J.M. Quinn and D.W. Murray, *J. Mater. Sci. Mater. Med.*, **12**, 659 (2001).
3. M. Ito, *Biomaterials*, **12**, 441 (1991).
4. L. Kong, Y. Gao, G. Lu, Y. Gong, N. Zhao and X. Zhang, *Eur. Polym. J.*, **42**, 3171 (2006).
5. Z. Feng, Y. Yuji, W.L. William, J. Chiyan Leong, Z. Wenyi, Z. Jingyu, Z. Mingfang and Y. Kangde, *Biomaterial*, **23**, 3227 (2002).
6. G. Chen and T. Ushida, *Biomaterials*, **22**, 2563 (2001).
7. L.D. Harris, D.F. Baldwin and D.J. Mooney, *J. Biomed. Mater. Res.*, **42**, 396 (1998).
8. Y.S. Nam and T.G. Park, *J. Biomed. Mater. Res.*, **47**, 8 (1999).
9. S.V. Madihally and H.W.T. Matthew, *Biomaterials*, **20**, 1133 (1999).
10. N. Pramanik, P. Bhargava, S. Alam and P. Pramanik, *Polym. Compos.*, **27**, 633 (2006).
11. M. Boissiere, P.J. Meadows, R. Brayner, C. Helary, J. Livage and T. Coradin, *J. Mater. Chem.*, **16**, 1178 (2006).
12. K. Kawagoe, M. Saito, T. Shibuya, T. Nakashima, K. Hino and H.J. Yoshikawa, *Biomed. Mater. Res.*, **53**, 678 (2000).
13. J. Li, Y. Zuo, X. Cheng, W. Yang, H. Wang and Y. Li, *J. Mater. Sci. Mater. Med.*, **20**, 1031 (2009).
14. M. Darder, M. Lo´pez-Blanco, P. Aranda, A.J. Aznar, J. Bravo and E. Ruiz-Hitzky, *Chem. Mater.*, **18**, 1602 (2006).
15. Y. Zhang and J.L.A. Mild, *Cryst. Growth Design*, **8**, 2101 (2008).
16. D.Z. Chen, C.Y. Tang, K.C. Chan, C.P. Tsui, P.H.F. Yu, M.C.P. Leung, and P.S. Uskokovic, *Compos. Sci. Technol.*, **67**, 1617 (2007).
17. F.E. Wiria, C.K. Chua, K.F. Leong, Z.Y. Quah, M. Chandrasekaran and M.W. Lee, *J. Mater. Sci. Mater. Med.*, **19**, 989 (2008).
18. Y. Pan and D. Xiong, *Wear*, **266**, 699 (2009).
19. M. Wang, Y. Li, J. Wu, F. Xu, Y. Zuo and J.A. Jansen, *J. Biomed. Mater. Res., Part A*, **85**, 418 (2008).
20. A. Costache, I. Pasuk, F. Ungureanu, A. Dinischiotu, F. Huneau, S. Galaup, P. Le Coustumer and D. Predoi, *Digest. J. Nanomater. Biostruct.*, **5**, 989 (2010).
21. K.S.V.K. Rao, K.M. Rao, P.V.N. Kumar and I.-D. Chung, *Iranian Polym. J.*, **19**, 265 (2010).
22. I. Manjubala, S. Scheller and J. Bossert, *Acta Biomater.*, **2**, 75 (2006).
23. L. Jiang, Y. Li, X. Wang, L. Zhang, J. Wen and M. Gong, *Carbohyd. Polym.*, **74**, 680 (2008).
24. J. Zhan, Y.H. Tseng, J.C.C. Chan and C.Y. Mou, *Adv. Funct. Mater.*, **15**, 2005 (2005).
25. S. Magaldi, S. Mata-Essayag, C.H. de Capriles, C. Perez, M.T. Colella, C. Olaizola and Y. Ontiveros, *Int. J. Infect. Disease*, **8**, 39 (2004).
26. R. Gandhidasan, A. Thamaraichelvan and S. Baburaj, *Fitoterapia*, **62**, 81 (1991).
27. A. Larena, D.A. Caceres and G. Ramos-Ortiz, *The Open Tissue Eng. Regenerat. Med. J.*, **2**, 40 (2009).